

MEAN-SPEED MEASUREMENTS IN TWO-DIMENSIONAL, INCOMPRESSIBLE,
FULLY-DEVELOPED TURBULENT CHANNEL FLOW

Thesis by
George Tolmie Skinner

In Partial Fulfillment of the Requirements
for the Degree of
Aeronautical Engineer

California Institute of Technology
Pasadena, California

1951

SUMMARY

Mean velocity profiles were measured in the 5" x 60" wind channel of the turbulence laboratory at the GALCIT, by the use of a hot-wire anemometer. The repeatability of results was established, and the accuracy of the instrumentation estimated. Scatter of experimental results is little, if any, beyond this limit, although some effects might be expected to arise from variations in atmospheric humidity, no account of this factor having been taken in the present work. Also, slight unsteadiness in flow conditions will be responsible for some scatter.

Irregularities of a hot-wire in close proximity to a solid boundary at low speeds were observed, as have already been found by others.

That Karman's logarithmic law holds reasonably well over the main part of a fully developed turbulent flow was checked, the equation $\frac{u}{u_\tau} = 6.0 + 6.25 \log_{10} \frac{y u_\tau}{z}$ being obtained, and, as has been previously the case, the experimental points do not quite form one straight line in the region where viscosity effects are small. The values of the constants for this law for the best over-all agreement were determined and compared with those obtained by others.

The range of Reynolds numbers used (based on half-width of channel) was from 20,000 to 60,000.

ACKNOWLEDGEMENTS

The author takes pleasure in acknowledging the advice and encouragement given, at all times, so readily by Dr. Hans W. Liepmann throughout the work reported here. The willingness of several of the students in the Department to argue out a dubious point is much appreciated, and, in particular, the unfailing ability of Satish Dhawan to detect a rash assumption helped avoid many pitfalls.

In the preparation of the manuscript, the able assistance of Mrs. Beverley Cottingham is gratefully acknowledged.

TABLE OF CONTENTS

Acknowledgements	
Summary	
Introduction	1
I Equipment and Methods	3
1. Channel	3
2. Traversing Mechanism	3
3. Calibration Tunnel	4
4. Hot-Wire	5
5. Measuring Equipment	6
List of Symbols	9
II Checks on the Two Dimensionality of the Channel Flow	11
III Choice of Operating Conditions for the Hot-Wire	15
IV Analysis of Experimental Accuracy	17
1. Resistance	17
2. Wire Temperature	18
3. Temperature Differential	18
4. Velocity	19
5. Current	20
6. Hot-Wire Constants	21
7. Slope of Velocity Profile at the Wall	23
8. Repeatability of Velocity Measurements	24
V Results and Discussion	26
List of Instruments	29
References	30

INTRODUCTION

Mean velocity measurements in both pipes and channels have been made from time to time by various investigators, particularly Nikuradse (Ref. 5), Dönch (Ref. 6), and Stanton (Ref. 7). Other authors have included mean speed measurements as part of their investigations. A certain amount of variation in experimental results has always existed and it seemed desirable to have a set of results coupled with some knowledge of the instrumentation accuracy. This at least enables one to decide whether or not a theoretical treatment of the problem adequately represents actual conditions, the final test of such a theory being that it should predict the mean velocity distribution in the channel. As other work on skin friction is being done in the GALCIT laboratories, the present results will enable a direct check to be made on the skin friction apparatus by measuring the actual shear stress at the wall of this channel, and comparing with the slopes of the velocity profiles at the wall.

Since most of the equipment necessary for such measurements already existed in the laboratory, it was decided to repeat the channel flow velocity profiles over the range of Reynolds numbers possible with the existing wind channel. A hot-wire probe was used to enable measurements to be taken as close to the wall as required for the accurate determination of $\left(\frac{du}{dy}\right)_0$, upon which rests the whole value of the logarithmic representation of the profiles.

It is perhaps doubtful if the same laws hold for both pipe and channel flows. It seems, therefore, worth while to check the channel

results again to compare them with those for flow in a circular pipe as given by other authors.

EQUIPMENT AND METHODS

1. Channel

Fig. 1 shows the complete tunnel layout. The channel, which is 60 inches high, starts with a width of 3 inches at the throat, and expands to 5 inches at a distance 7 feet downstream of the throat. This width is maintained for the remainder of the channel (over-all length from throat to exit is 23 feet). Approximately the last 6 feet of the channel is lined with highly polished birch. A full description of the tunnel appears in Ref. 1.

The slight variation in width between the walls is shown in Fig. 6.

A natural gas engine drives the impeller and it was possible to reach a Reynolds number of slightly over 70,000 (based on the half-width of the channel). However, because of trouble with the engine, it was not possible to repeat the 70,000 Reynolds number set of measurements in the final runs. The lower limit of stable operation was near a Reynolds number of 20,000.

2. Traversing Mechanism

The existing micrometer traverse was used. This has a coarse adjustment in 2.5 cm. steps, and micrometer adjustment over 2.5 cms. with 0.001 cm. graduations. The principle of taking up backlash was observed in all measurements, the slide being brought up to its setting by drawing it towards the wall in every case.

The zero position of the wire was found by removing one side of

the 6 inch extension on the exit of the channel and bringing a microscope to focus on the wire while a focussed beam of light was thrown on the wire in a direction as nearly parallel to the wall as possible. A sharp reflection is returned from the wire, and a slightly less sharp image is formed in the wall, which is kept highly polished for this purpose. By using a calibrated eyepiece in the microscope, the distance between the reflection from the wire and its image in the wall is found. This, divided by two, is almost exactly the distance between the wire and the wall. The zero was calculated for several settings of the wire, and all were found to agree to less than 0.001 cm. The method is that used by Laufer in his work on the same channel. With the 0.0005 inch diameter wires used for mean speed measurements, it is a little more difficult to find the zero than with the very fine wires used for turbulence measurements, since the wire is sufficiently thick to cause a slight discrepancy between the orientation of the reflection from the wire itself and the image reflection.

By trial and error, the wire can be set accurately parallel to the wall, using the microscope each time to measure the distance between wire and image at both top and bottom of the wire. In determining the zero position, the center of the wire was used.

3. Calibration Tunnel

For calibration of the wire, the isotropic turbulence tunnel was used, normally without screens in place, although checks have been made to ensure that the calibration is not measurably altered

by the presence of turbulence. Since the values of u'/u become large at some points of the channel, the calibration might be expected to be invalidated. However, the linearized correction is so small that it may be neglected. As such levels of turbulence are not reproducible in the calibration tunnel, no further checks could be made in this direction. A diagram and description of this tunnel appear in Ref. 2.

4. Hot-Wire

To obtain good sensitivity coupled with reasonable mechanical strength, a wire of 2.5 cms. length and 0.0005 inch diameter was used. All the final results were made with the same wire, although others were used in earlier parts of the work, including a shorter wire of about 1 cm. length which lacked the necessary sensitivity. At first it might appear that with a 2.5 cms. wire, irregularities in the channel wall would cause errors when the wire is very close to it; however, inspection with the microscope showed the wall to be adequately plane for a constant distance to exist between wall and wire throughout the whole length of the wire.

The finest sewing needles were used to form the wire support. The wire itself was wrapped around the points in such a fashion as to allow it to be brought as close as desired to the wall. The supporting needles were set pointing slightly towards the wall to assist in this matter.

Platinum wire was used and was attached to the needles by soft-soldering. Frequent cleaning in ether ensured cleanliness.

The wire used for the final velocity profiles was made up, calibrated and used within the space of two days, in order to ensure no physical change. Calibration included determination of the temperature coefficient of resistance (Fig. 8).

Constant sensitivity was achieved by using the constant resistance method of operation.

5. Measuring Equipment (Circuit, Fig. 2)

The hot-wire occupied one arm of a Wheatstone Bridge. The heating current of the wire was therefore the current through that branch of the circuit. A commercial bridge was used (see appended list of instruments) and the ranges were selected so as not to exceed the current limitations of the bridge.

A panel of variable resistances, together with a selection of fixed resistances for low current readings, was mounted above the bridge in a rack. The variables were 1,000 Ω ; 100 Ω ; 1 Ω chosen with the requisite number of turns to their windings to give complete coverage. Normally only the 100 Ω and 1 Ω resistances are in circuit. The 1 Ω had over 60 turns. This gave adequately fine adjustment throughout using wires of about 20 Ω "cold" resistance. A 6 volt lead storage battery was used for heating. In the author's opinion it is not desirable to use a high voltage source with a large series resistance, as this tends to maintain constant current, and deviations in resistance could not be noticed while current readings were being taken. Furthermore, as a drop in resistance causes an increase in current, which tends to maintain constant resistance, and vice versa,

nothing is lost by using a low voltage source and low series resistance. With the arrangement used, current readings were nevertheless much more stable than resistance settings.

In order to measure current, a 1Ω standard resistance was placed in series with the hot-wire and its leads. The voltage across the 1Ω standard was then numerically equal to the current through the hot-wire, and was read on a precision potentiometer. It was found that the resistance of the leads (which were no longer than necessary, about 8 feet) remained constant to considerably greater accuracy than was required over the current range used. Short lengths of fine wire on the end of a shielded cable were used for attachment to the probe. These were fine enough to ensure no movement of the probe due to forces arising from the leads. All joints were soldered within the bridge circuit, and attachment of the cable and 1Ω standard was from behind the panel, the wires being soldered to the back of the normal terminals for the "unknown" resistance.

The same galvanometer was used for both bridge and potentiometer. Switching was provided where necessary and the change from current measurement to bridge balancing could be made in a fraction of a second. Where unsteadiness in the flow caused periodic large deviations, both balance points usually could be checked during the quiescent periods.

The potentiometer for current measurements was left with current passing through it at all times, except when it was necessary to check batteries. Actually, during most of the work the circuit was never broken.

A motor driven alcohol manometer of the Zahn type calibrated to 0.001 cm. was used. A light was attached to the meniscus carriage to avoid parallax errors. No heating errors were observed.

The whole equipment, including power supplies, was mounted on a heavy trolley so that it could be moved, en masse, to the calibration tunnel when required. An hour or so was necessary for the standard cell to settle down after being moved (it was normally moved separately) although the deviation was very slight immediately after moving.

LIST OF SYMBOLS

- x = distance upstream of point at which probe support enters channel (channel exit equal to $-5 \frac{7}{8}$ inches)
- y = horizontal distance from channel wall
- z = distance vertically above center of channel

In the theoretical discussion under "Checks on the Two Dimensionality of the Channel flow," x refers to the downstream direction.

- d = half width of channel = 2.50 inches = 6.35 cms.
- u = mean velocity parallel to x axis
- u_0 = mean velocity parallel to x axis at center of channel
- u' = velocity fluctuation in x direction (as used in theoretical discussion)
- v' = velocity fluctuation in y direction (as used in theoretical discussion)
- w' = velocity fluctuation in z direction (as used in theoretical discussion)
- $\left(\frac{du}{dy}\right)_0$ = slope of velocity profile at the wall
- u_τ = "friction velocity" = $\sqrt{\frac{\tau}{\rho}} = \sqrt{\frac{\mu \left(\frac{du}{dy}\right)_0}{\rho}}$
- p = static pressure
- ρ = air density
- ρ_m = manometer alcohol density
- μ = absolute air viscosity
- ν = kinematic air viscosity

- Δp = difference between static pressure and atmospheric pressure
 q = dynamic pressure
 h = manometer head (cms. of alcohol)
 R.N. = Reynolds number based on half-width of channel
 α = temperature coefficient of resistance of the hot-wire
 θ = temperature of hot-wire ($^{\circ}\text{C}$)
 θ_a = local air temperature ($^{\circ}\text{C}$)
 R = resistance of hot-wire at temperature θ
 R_0 = resistance of hot-wire at 0°C
 i = hot-wire current (amps.)
 a, b = constants of King's equation

Fractional Errors:

$$\epsilon_i = \frac{di}{i} ; \quad \epsilon_R = \frac{dR}{R} ; \quad \epsilon_u = \frac{du}{u} ; \quad \epsilon_{\theta} = \frac{d(\theta - \theta_a)}{(\theta - \theta_a)} .$$

CHECKS ON THE TWO DIMENSIONALITY OF THE CHANNEL FLOW

Starting with Reynold's equation

$$\rho u_k \frac{\partial u_i}{\partial x_k} = \frac{\partial p_{ik}}{\partial x_k} \quad (1)$$

and the continuity equation

$$\frac{\partial u_i}{\partial x_i} = 0 \quad (2)$$

Most of the terms in the stress tensor, p_{ik} , drop out when the two-dimensional channel flow conditions are imposed (cf. Ref. 1). Taking time averages of the fluctuating quantities and assuming p independent of the direction normal to the mean velocity vector and parallel to the channel wall leads to the following two equations:

$$\frac{\partial}{\partial x} (-p - \overline{\rho u'^2}) + \frac{\partial}{\partial y} (\mu \frac{du}{dy} - \rho \overline{u'v'}) = 0 \quad (3)$$

$$\frac{\partial}{\partial y} (-p - \overline{\rho v'^2}) + \frac{\partial}{\partial x} (\mu \frac{du}{dy} - \rho \overline{u'v'}) = 0 \quad (4)$$

For fully developed flow, $\overline{u'^2}$, $\overline{v'^2}$, $\overline{u'v'}$, u , $\frac{du}{dy}$ are all independent of x , the direction parallel to the mean velocity vector. Thus, the above equations reduce to

$$-\frac{\partial p}{\partial x} + \mu \frac{d^2 u}{dy^2} - \rho \frac{d}{dy} (\overline{u'v'}) = 0 \quad (5)$$

and

$$-\frac{\partial p}{\partial y} - \rho \frac{d}{dy} (\overline{v'^2}) = 0 \quad (6)$$

Differentiation of Eq. (6) with respect to x gives

$$\frac{1}{\rho} \frac{\partial^2 p}{\partial x \partial y} = \frac{\partial}{\partial x} \left(-\frac{\partial \overline{v'^2}}{\partial y} \right)$$

which equals zero, since $\overline{v'^2}$, and therefore $\frac{\partial \overline{v'^2}}{\partial y}$, are independent of x . Also, we note that $\frac{dp}{dx} = \text{constant}$. Hence Eq. (5) can be integrated with respect to y :

$$\frac{y}{\rho} \left(\frac{dp}{dx} \right) = \nu \frac{du}{dy} - \overline{u'v'} + \text{constant} \quad (7)$$

Now, total shear vanishes at the center of the channel ($y=d$), i.e.

$$\nu \frac{du}{dy} - \overline{u'v'} = 0$$

$$\therefore \text{constant} = \frac{d}{\rho} \left(\frac{dp}{dx} \right)$$

Eq. (7) therefore becomes:

$$\frac{y-d}{\rho} \cdot \frac{dp}{dx} = \nu \frac{du}{dy} - \overline{u'v'} \quad (8)$$

Since $\frac{dp}{dx} = \text{constant}$, the total shearing stress is a linear function of y .

At the wall, the shearing stress is given entirely by the viscous term, since v' must go to zero.

$$\therefore \frac{d}{\rho} \left(-\frac{dp}{dx} \right) = \nu \left(\frac{du}{dy} \right)_0 = \tau_0$$

Hence, we can obtain a check by measuring $\frac{dp}{dx}$ and $\nu \left(\frac{du}{dy} \right)_0$. However, $\frac{dp}{dx}$ is so small that this check is of little value. Nevertheless, it was necessary to use the fact that $\frac{dp}{dx}$ should be constant to help establish the assumption of two dimensionality of the flow. Measurements of $\frac{dp}{dx}$ showed a generally steady rate of change of

pressure, but the channel does suffer from a "kink" in the pressure gradient. The measurements at $y = d/2$ show deviations from a straight line similar to those at mid-channel.

To measure pressure gradients, the manometer was fitted with its microscope attachment and readings of pressure were taken from the hair-line micrometer screw. The lines to the two sides of the manometer included lengths of thin rubber tubing for damping purposes (the lengths were adjusted to eliminate errors from pressure fluctuations in the building). Results proved to be quite repeatable.

The static tube used was a long brass tube of $7/16$ inch diameter with a $1/8$ inch extension, $7\ 1/2$ inches long, fitted to the nose. The whole arrangement was held in a stand externally and the base levelled with a spirit level. The tube was then adjusted to bring the thin extension horizontal, by sighting on a line marked on the laboratory wall. Once levelled for any given amount of overhang of the static tube, the stand could be slid towards the tunnel exit until the static holes were at the required position, when the base could once again be brought to a level position by means of the spirit level. Measurements were made at the center of the channel and at $y = d/2$, opposite the hot-wire measuring position (Fig. 3). The static tube was checked in a free jet and was found to read atmospheric pressure within 1.3% of the maximum speed used.

The other checks on two dimensionality were based on quantities which should remain constant in a direction parallel to the channel axis. As no turbulence measurements could be made, reference is given to Laufer's report (Ref. 1) where he shows that although $\frac{\partial u^2}{\partial x}$ is

not zero, it is small compared with $\frac{1}{\rho} \frac{dp}{dx}$ (see Eq. (3), et seq of this report).

Velocity profiles were taken at various positions along the x axis and the fact that these remain constant, shows that the flow is indeed sufficiently two-dimensional. A sample set of curves is given in Fig. 5.

As noted in the description of the channel, a slight variation in width exists. This is shown in Fig. 6. Since the fluctuations in width match the fluctuations in $\frac{dp}{dx}$, a check was made to see if the width variation could account for this change. Basing the argument on one-dimensional considerations

$$Q = Au_m = \text{constant} \quad (\text{where } Q \text{ is the total flux and } u_m = \text{mean velocity})$$

(A = cross-sectional area of channel)

$$\therefore \frac{du_m}{u_m} = -\frac{dA}{A}$$

$$\text{Also } p + \frac{1}{2} \rho u_m^2 = \text{constant}$$

$$\therefore dp = -\left(\frac{1}{2} \rho u_m^2\right) \left(2 \frac{du_m}{u_m}\right) = +q \frac{2dA}{A} \text{ where } q = \frac{1}{2} \rho u_m^2 .$$

The total cross-sectional area, and changes in it, were used for this calculation, and the correct pressure readings showed some slight improvement, but did not become straight lines. However, with the low pressure gradients in use, this is probably not serious.

It should be noted that the logarithmic law for the velocity profile is based on no pressure gradient conditions, and, in the presence of slight such gradients, is treated as a first approximation (see, e.g. Ref. 3, Vol. II, p. 333).

CHOICE OF OPERATING CONDITIONS FOR THE HOT-WIRE

Three parameters can be varied in order to alter the operating conditions of a hot-wire; viz.: length, diameter, temperature difference between wire and air-stream.

First it is necessary to have a wire of sufficient length to give a reasonable absolute change of resistance with velocity. Length is limited by mechanical considerations, and 2.5 cms. was found to be a good compromise, in conjunction with a diameter of 0.0005 inches.

Having decided on these physical conditions, it is necessary to check that the percentage change in velocity over a distance of 0.0005 inches in the laminar sub-layer is not too great at the highest Reynolds numbers to be used. At R.N. = 60,000, $\left(\frac{du}{dy}\right)_0 = 21,500$ (cms./sec.)/cm. Therefore for $dy = 0.0005$ inch

$$du = 21,500 \times 0.0005 \times 2.54 = 27.3 \text{ cms./sec.}$$

To check this at the center of the laminar sub-layer, we take $u \doteq 250$ cms./sec. Thus $\frac{du}{u} \doteq 11\%$.

At a Reynolds number of 20,000 this figure has dropped to 0.4%.

This, at least, gives some idea of the relationship between the size of the wire and the velocity gradients to be measured.

Sensitivity and accuracy are much dependent upon the temperature difference between the wire and the air-stream. However, conduction to the walls of the channel becomes serious when the wire is close to the wall, if this temperature difference is not held to a minimum.

It should first be noted that conduction to the walls is not very much more serious with a thick wire than with a thin wire. At

zero air velocity, the effect of conduction to the channel walls was noticeable at distances of about 0.1 inch. (Being of wood, the walls had about as low a thermal conductivity as possible.) This effect suggested that the wire might be calibrated and operated at various temperatures and the most suitable temperature for operation in the laminar sub-layer determined. With a temperature difference of 5°C , it was found that fluctuations in room temperature would almost completely invalidate readings. Also, at differences in the range 5°C to 20°C , the lack of sensitivity of the circuits was sufficient to give the impression that the wire read higher than the true velocity. However, from 20°C to 50°C velocity profiles in this region checked sufficiently well to suggest that a temperature differential of 40°C would be suitable. This check was made at $R.N. = 20,000$ because at low speeds there is the greatest possibility of error.

One set of measurements is shown in Fig. 7, where it can be seen that the readings reach a minimum at about 40°C and show a tendency to rise as the temperature is raised further. At this Reynolds number the laminar layer extends to about 0.04 cm.

ANALYSIS OF EXPERIMENTAL ACCURACY

Since the hot-wire was calibrated under approximately the same conditions as those under which it was used, it was necessary only to assume that King's equation holds over a narrow region in the vicinity of the calibration conditions. However, it was not possible to calibrate for velocities lower than about 4 meters/sec. as here errors in pitot-static measurements are liable to become large. Hence, it is assumed that the calibration line may be extended to zero. Owing to air currents set up by the wire, the zero velocity point cannot be determined sufficiently accurately. Further, when the intensity of the velocity fluctuations becomes high, the wire reads velocities below the true mean. An approximate correction for this is given in Ref. 1: $u_{\text{wire}} = \bar{u} \left[1 - \frac{3}{16} \left(\frac{u'}{\bar{u}} \right)^2 + \dots \right]$. This correction was made on the basis of Laufer's velocity fluctuation measurements and found to amount to about 1.5% at the point where the ratio of fluctuation velocity to local mean velocity was highest. The correction was therefore not applied to subsequent measurements.

The following estimate of experimental accuracy is based on the use of King's equation (Ref. 4), $\frac{i^2 R}{\theta - \theta_a} = (a + b\sqrt{u})$.

1. Resistance

With the Wheatstone Bridge used, resistances of 20 Ω can be measured to four significant figures. The 2.5 cms. hot-wires have a resistance of around 20 Ω , so that the accuracy of resistance measurement is 0.05%.

2. Wire Temperature

Wire temperatures were based on a knowledge of the wire resistance at 0 °C and at the temperature in question, $\left[\theta = \frac{R - R_0}{\alpha R_0} \right]$. α was measured by immersing the wire in a bath of distilled water or oil and taking resistance readings at small currents for temperatures covering the range used. α is thus known to the degree of accuracy of temperature measurement (0.1 C°) combined with that of resistance measurement. At the lower end of the temperature scale (25 °C) temperature is thus known to 0.4%. Resistance accuracy is ten times as great and so α is known essentially to 0.4%. Incidentally, the usual value of 0.0037 for α was found not to hold for the platinum wire used, α being 0.00341. (A wire which had been used for some time gave $\alpha = 0.00343$.) Thus it would appear to be desirable to measure this quantity for each wire. $(R - R_0)$ is known to 0.225% (0.01 Ω) at temperatures of about 65 °C. In operation the "hot" resistance of the wire was kept always at the same value and was, in fact, taken directly from the curve from which α was determined. Hence, θ is really known to the accuracy of the temperature readings, i.e. 0.1 C°.

3. Temperature Differential

From the preceding paragraph and the fact that temperatures could be read to 0.1 C°, $(\theta - \theta_a)$ was known to 0.2 C°. Usually the thermometer was read to the nearest 1/20 C° but it is not assumed that temperatures are really as accurate as the above would indicate. As $(\theta - \theta_a)$ was always very nearly 40 C°, this quantity is known to 0.5%.

During velocity calibration, a thermometer was placed in the tunnel. The stagnation rise is given by $\frac{T}{T_0} \doteq 1 - \frac{\gamma-1}{2} M^2$ and amounts to 0.1° at 1430 cms./sec. From a consideration of the large scale velocity calibration line, it is apparent that there was no point in correcting for this.

During velocity profile measurements the thermometer was hung near the channel exit, a few inches from the wire position. It had been found that holding the thermometer in the channel exit gave no detectable difference in reading. Again no correction was made for local air temperature at the wire.

4. Velocity

The calibration tunnel will hold its dynamic head steadily to the accuracy of the manometer readings without trouble. The channel, if the engine is allowed the requisite period for warm-up, will do like-wise over reasonably long periods. As far as possible, every effort was made to stabilize conditions in order to eliminate frequent adjustments of speed. The manometer can be read with ease to 0.002 cm. alcohol, and as the small light on the meniscus-tube moves with the slide, no parallax errors are introduced. Prolonged use of the manometer showed that no error was introduced by heating of the fluid.

$$\text{Now } \frac{1}{2} \rho u^2 = \rho gh \quad \therefore \frac{du}{u} = \frac{1}{2} \frac{dh}{h}$$

$$\text{At R.N.} = 60,000 \quad h \doteq 1.7$$

$$\therefore \frac{du}{u} = \frac{1}{2} \times \frac{0.002}{1.7} = 0.0006 \text{ or } 0.06\%$$

$$\text{At R.N.} = 20,000 \quad h \doteq 0.18$$

$$\therefore \frac{du}{u} = \frac{1}{2} \times \frac{0.002}{0.18} = 0.006 \text{ or } 0.6\%$$

Similarly, changes in air density and alcohol density may cause further errors in velocity readings. These errors are of the order of 0.07% and 0.03%, respectively; and so, at the lower speeds may be neglected in comparison with the above. At the highest speeds, therefore, the total possible velocity error is of the order of 0.16% and so is negligible; while at the lower speeds the total of 0.7% is acceptable.

Velocities were only held constant in the channel by use of the pitot-static tube as about 1% error is introduced by the $\overline{u^2}$ term in the root mean square velocity and a further error may be introduced since, even with the small pitot-static heads normally used, the distance between the pitot and static openings is sufficient to cause a 1% or 2% error. Actually, a special rig was made with a pitot tube (hypodermic needle with squared-off end) lined up opposite the static holes, so that $\frac{dp}{dx}$ would not introduce this error. Although agreement is reasonable between hot-wire and manometer readings at the center of the channel, this pitot-static combination has not been carefully calibrated and so reliance is not placed on its readings.

5. Current

Potentiometer voltage readings are possible to at least 2×10^{-5} volts. This varies, of course, with the steadiness of the reading, but during calibration, readings of current are very steady, and most errors are introduced as a result of fluctuations in the wire temperature while in the channel, particularly when measuring in the

transition region between the laminar boundary layer and the completely turbulent region. In this region the turbulence level is unsteady and the mean speed fluctuates sufficiently to make accurate readings difficult to obtain. Nevertheless, readings check fairly well in repeated measurements. An error of 2×10^{-5} volts represents 0.04% accuracy at the lowest currents used.

The 1Ω standard which provides this voltage is a 0.02% resistance. Thus, total error amounts to 0.06%.

6. Hot-Wire Constants

For the purpose of determining the instrument errors arising in the wire constants (a and b) the following notation will be used:

$$\begin{array}{llll} \text{Maximum possible error in } u & = du & \text{and } \left| \frac{du}{u} \right| & = \epsilon_u \\ \text{Maximum possible error in } R & = dR & \text{and } \left| \frac{dR}{R} \right| & = \epsilon_R \\ \text{Maximum possible error in } i & = di & \text{and } \left| \frac{di}{i} \right| & = \epsilon_i \\ \text{Maximum possible error in } (\theta - \theta_a) & = d(\theta - \theta_a) & \text{and } \left| \frac{d(\theta - \theta_a)}{(\theta - \theta_a)} \right| & = \epsilon_\theta \end{array}$$

where u , R , i , and $(\theta - \theta_a)$ are the measured quantities. Substituting in King's equation:

$$\frac{i^2 R}{\theta - \theta_a} \left[\frac{(1 \pm 2\epsilon_i)(1 \pm \epsilon_R)}{(1 \pm \epsilon_\theta)} \right] = a + b\sqrt{u} (1 \pm \frac{1}{2}\epsilon_u),$$

neglecting higher powers of ϵ . The correction factor on the left may be written:

$$(1 \pm 2\epsilon_i)(1 \pm \epsilon_R)(1 \mp \epsilon_\theta + \dots) = (1 \pm 2\epsilon_i \pm \epsilon_R \mp \epsilon_\theta)$$

Thus the worst fractional error in $\frac{i^2 R}{\theta - \theta_a}$ is given by

$$(2\epsilon_i + \epsilon_R + \epsilon_\theta) = (\text{say}) \epsilon_1. \quad (\text{since signs may be chosen arbitrarily})$$

Rearranging,

$$a = \frac{i^2 R}{\theta - \theta_a} (1 \pm \epsilon_1) - b \sqrt{u} (1 \pm \frac{1}{2} \epsilon_u)$$

$$\therefore \frac{da}{a} = \frac{1}{a} \left[\frac{\partial a}{\partial (\frac{i^2 R}{\theta - \theta_a})} \cdot \frac{\epsilon_1 i^2 R}{\theta - \theta_a} + \frac{\partial a}{\partial \sqrt{u}} (\pm \frac{1}{2} \epsilon_u) \sqrt{u} \right]$$

So:

$$\frac{da}{a} = \frac{1}{a} \left[(1 \pm \epsilon_1) \frac{\epsilon_1 i^2 R}{\theta - \theta_a} + b (1 \pm \frac{1}{2} \epsilon_u) \frac{1}{2} \epsilon_u \sqrt{u} \right]$$

or

$$\frac{da}{a} = \frac{1}{a} \left[\epsilon_1 \frac{i^2 R}{\theta - \theta_a} + \frac{b \epsilon_u \sqrt{u}}{2} \right]$$

neglecting higher orders of ϵ .

Similarly

$$\frac{db}{b} = \frac{1}{2b\sqrt{u}} \left[\frac{i^2 R}{\theta - \theta_a} (\epsilon_u + 2\epsilon_1) + a \epsilon_u \right]$$

Taking values for the middle of the velocity range used,

$$\epsilon_u = 0.003$$

$$u = 900 \text{ cms./sec.}$$

$$\epsilon_\theta = 0.005$$

$$\epsilon_R = 0.0005$$

$$\epsilon_i = 0.00025$$

$$\therefore \epsilon_1 = 0.006$$

$$a = 9.0 \times 10^{-4} = 10^{-3}$$

$$b = 0.9 \times 10^{-4} = 10^{-4}$$

$$\frac{i^2 R}{\theta - \theta_a} = 36 \times 10^{-4}$$

$$\begin{aligned} \therefore \frac{da}{a} &= 10^3 \left(0.006 \times 36 \times 10^{-4} + 10^{-4} \times 0.003 \times \frac{30}{2} \right) \\ &= 0.0216 + 0.0045 = 0.026 \text{ or } \underline{2.6\%} \end{aligned}$$

and $\frac{db}{b} = 0.009 = 0.9\%$.

It was noticed during early velocity calibrations where temperature was measured only to $1/2^\circ \text{C}$, that b did not change noticeably, while there was about 10% fluctuation in a . With a five-fold improvement in temperature accuracy the above results are to be expected.

7. Slope of Velocity Profile at the Wall

Since the accuracy of the semi-logarithmic plots of the velocity profiles rests almost completely upon the values of $\left(\frac{du}{dy}\right)_0$, it will be of interest to estimate the accuracy with which this quantity can be measured. For this purpose, the value of the velocity at the limit of the laminar sub-layer will be taken, and the maximum possible instrumentation error calculated for this, together with an assumed maximum error of 0.0005 cm. in the measurement of y . Details are as follows: (Note: velocity is calculated thus: $\sqrt{u} = \frac{1}{b} \left(\frac{i^2 R}{\theta - \theta_a} - a \right)$ and so is principally dependent on "a".)

R.N.	= 20,000	30,000	45,000	60,000
u (limit of laminar sub-layer)	= 140	200	300	400 cms./sec.
y (limit of laminar sub-layer)	= 0.050	0.033	0.025	0.020 cms.

$$\left(\frac{i^2 R}{\theta - \theta_a} - a \right) \times 10^4 = 10.7 \quad 13 \quad 16 \quad 18$$

$$\left(\frac{da}{\frac{i^2 R}{\theta - \theta_a} - a} \right) = \frac{d\sqrt{u}}{\sqrt{u}} = 0.021 \quad 0.018 \quad 0.014 \quad 0.013$$

(a has been taken as 9.00 and corresponds to the wire used for final

measurements.)

Hence	$\frac{du}{u}$	=	0.042	0.056	0.028	0.026
and	$\frac{dy}{y}$	=	<u>0.010</u>	<u>0.015</u>	<u>0.020</u>	<u>0.025</u>
			0.052	0.051	0.048	0.051
	percentage accuracy of $\left(\frac{du}{dy}\right)_0$	=	5.2%	5.1%	4.8%	5.1%

Now $u_z \sim \sqrt{\left(\frac{du}{dy}\right)_0}$, therefore, percentage accuracy of $u_z \doteq 2.5\%$ for all Reynolds numbers. The slope of the logarithmic plot is given by $\frac{\Delta(u/u_z)}{\Delta(yu_z/\nu)}$. If the main error occurs in u_z then the slope is subject to a possible error of approximately twice that of u_z (viz. 5%). Since the value of the slope is in the region of 6, the error may be ± 0.3 . Thus, from the present results the slope may be from 5.96 to 6.55.

8. Repeatability of Velocity Measurements

Although the accuracy of the absolute velocity readings depends on the wire constants (a and b), the repeatability depends only on the combined accuracy of the measurements of $\frac{i^2 R}{\theta - \theta_a}$ and the constancy with which dynamic pressure can be held.

We have, earlier,

$$\frac{du}{u} = \frac{1}{2} \frac{dh}{h} = \begin{cases} 0.06\% \text{ at R.N.} = 60,000 \\ 0.6\% \text{ at R.N.} = 20,000 \end{cases}$$

Also

$$\frac{d\left(\frac{i^2 R}{\theta - \theta_a}\right)}{\left(\frac{i^2 R}{\theta - \theta_a}\right)} = \epsilon, \quad = 0.6\% \text{ at the middle of the velocity range used}$$

As can be seen by a study of King's equation together with the

actual numbers encountered in these measurements, the error in velocity caused by ϵ_1 may range from $6 \epsilon_1$ in the sub-layer of the low speed flow to $1\frac{1}{4} \epsilon_1$ at the center of the high speed flow. This is in reasonable agreement with Figs. 12a and 12b where it is seen that the absolute error remains approximately constant between 10 and 20 cms./sec., which is slightly more than the instrument inaccuracies would indicate.

RESULTS AND DISCUSSION

The theoretical derivation of the logarithmic law for the velocity distribution near a wall, using the momentum transfer theory, is given in Ref. 3, Vol. 2.

By the introduction of the so-called "friction velocity," u_τ , the velocity profile may be expressed non-dimensionally by the equation

$$\frac{u}{u_\tau} = A + B \log_{10} \left(y \frac{u_\tau}{\nu} \right)$$

This equation is expected to be valid throughout the region in which viscous stresses may be neglected in comparison with the Reynolds stresses. From the semi-logarithmic plot (Fig. 11) it appears that the deviation occurs around $y \frac{u_\tau}{\nu} = 30$.

The equation $\frac{u}{u_\tau} = 6.00 + 6.25 \log_{10} y \frac{u_\tau}{\nu}$ gives a straight line on Fig. 11 which is in fairly good agreement with the experimental points. It is clear, however, that near the wall the slope has a tendency to be shallower and near the center of the channel the slope tends to be steeper.

The equation corresponding to the above, as given in Ref. 3 for the best over-all agreement with Nikuradse's results for circular pipes is $\frac{u}{u_\tau} = 5.5 + 5.75 \log_{10} y \frac{u_\tau}{\nu}$.

Diessler, (Ref. 9), obtains the equation

$$u^+ = \frac{1}{0.38} \log_e y^+ + 3.8$$

which in the present notation becomes

$$\frac{u}{u_\tau} = 3.8 + 6.40 \log_{10} y \frac{u_\tau}{\nu}$$

the slope being in good agreement with the present results.

Diessler's results are obtained from flows in smooth pipes over a range of Reynolds numbers from 8,000 to 200,000 based on tube diameter.

In the same channel as was used for the present report Laufer obtained the equation $\frac{u}{u_\tau} = 5.5 + 6.9 \log_{10} \frac{y u_\tau}{\nu}$. Wattendorf, who gives figures for both straight and curved channels, obtained a line for the straight part of his channel which had approximately the equation $\frac{u}{u_\tau} = 4 + 6 \log_{10} \frac{y u_\tau}{\nu}$.

It should also be mentioned that in the laminar sub-layer at the lowest Reynolds number (20,000) the hot-wire measures velocities lower than the true mean. This was also found by Laufer (Ref. 1). The fact that the points rise as the wall is approached very closely, is doubtless due to heat conduction to the wall. The linearized correction to the mean velocity for the presence of turbulence does not materially improve the sub-layer mean velocities. (Turbulence levels for this may be obtained from Laufer's results.) However, in drawing the profile near the wall, the curve must end, presumably, in a straight line without discontinuities in either slope or curvature. If one simply draws a curve through the measured points and from the origin extends a tangent to this curve, it is fairly clear that curvature becomes zero abruptly. Hence it seems reasonable to take a straight line which lies slightly above the measured points (except, of course, the first one) and which has a slope less than the maximum slope of the measured points. Both extremes were tried and in the logarithmic plot the points came first to one side and then to the other by about equal amounts. The above intermediate procedure gave

points on the logarithmic plot which check well with the other results.

Finally, as an indication of the reliability of absolute velocity measurements with a hot-wire, sets of measured points for the highest and lowest Reynolds numbers used are given in Figs. 12a and 12b. These points represent measurements made with steady atmospheric conditions during each individual run, (i.e., principally, temperature does not change by more than 0.5°). In order to get such steady conditions in this laboratory it was usually not possible to measure during the day, when temperature fluctuations tend to become serious. It should be noted that Figs. 12a and 12b were obtained with a wire whose constants were not known accurately; however, this does not impair the value of the curves as examples of repeatability of measurements, although their shape may be slightly in error.

LIST OF INSTRUMENTS

Wheatstone Bridge: Shallcross Wheatstone-Kelvin Bridge, Model
No. 638-2

Potentiometer: Leeds and Northrup, Model No. 7552

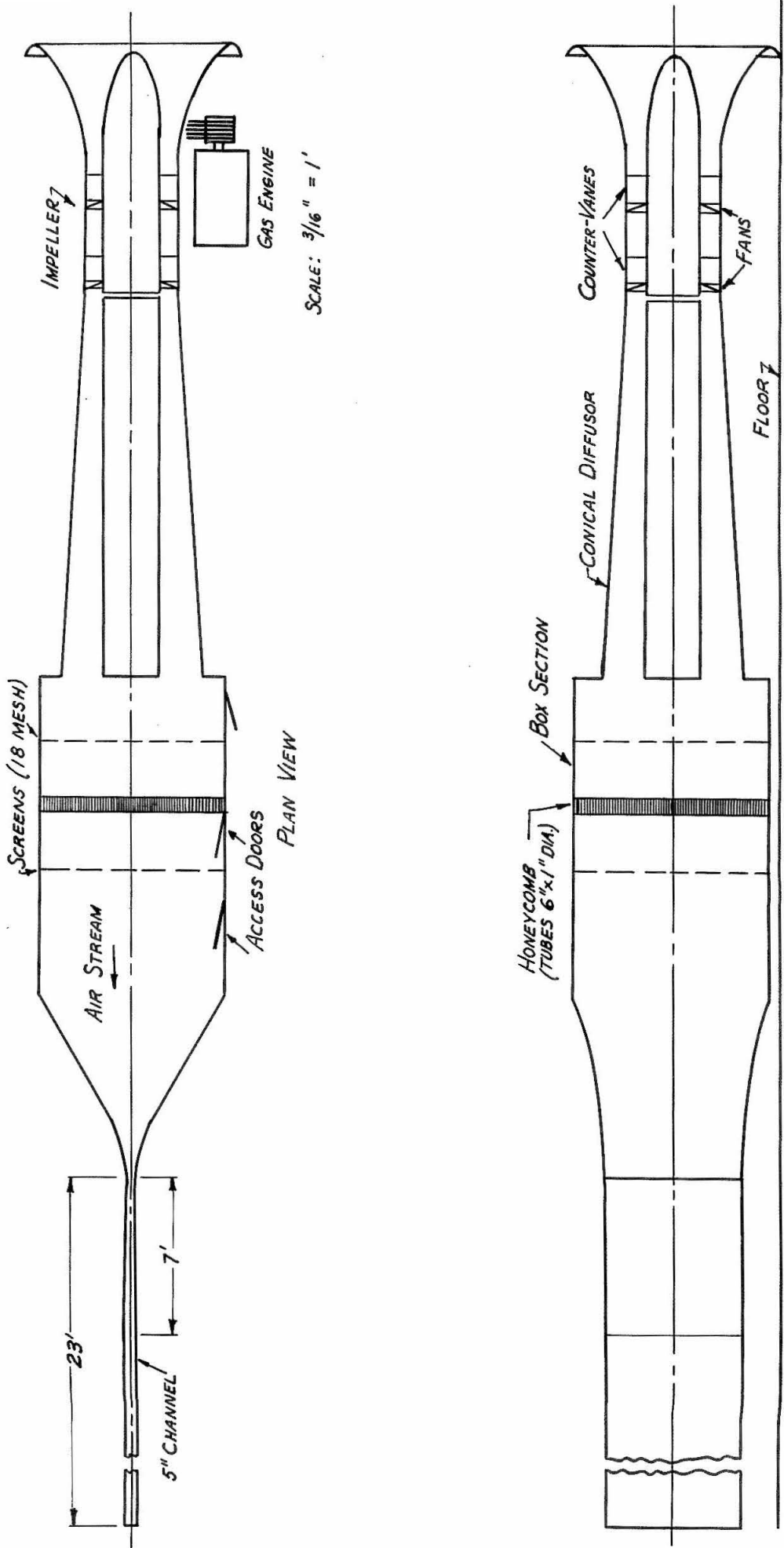
Galvanometer: Leeds and Northrup, Model No. 2420 B

1 Ω Standard: Shallcross 1 international $\Omega \pm 0.02\%$

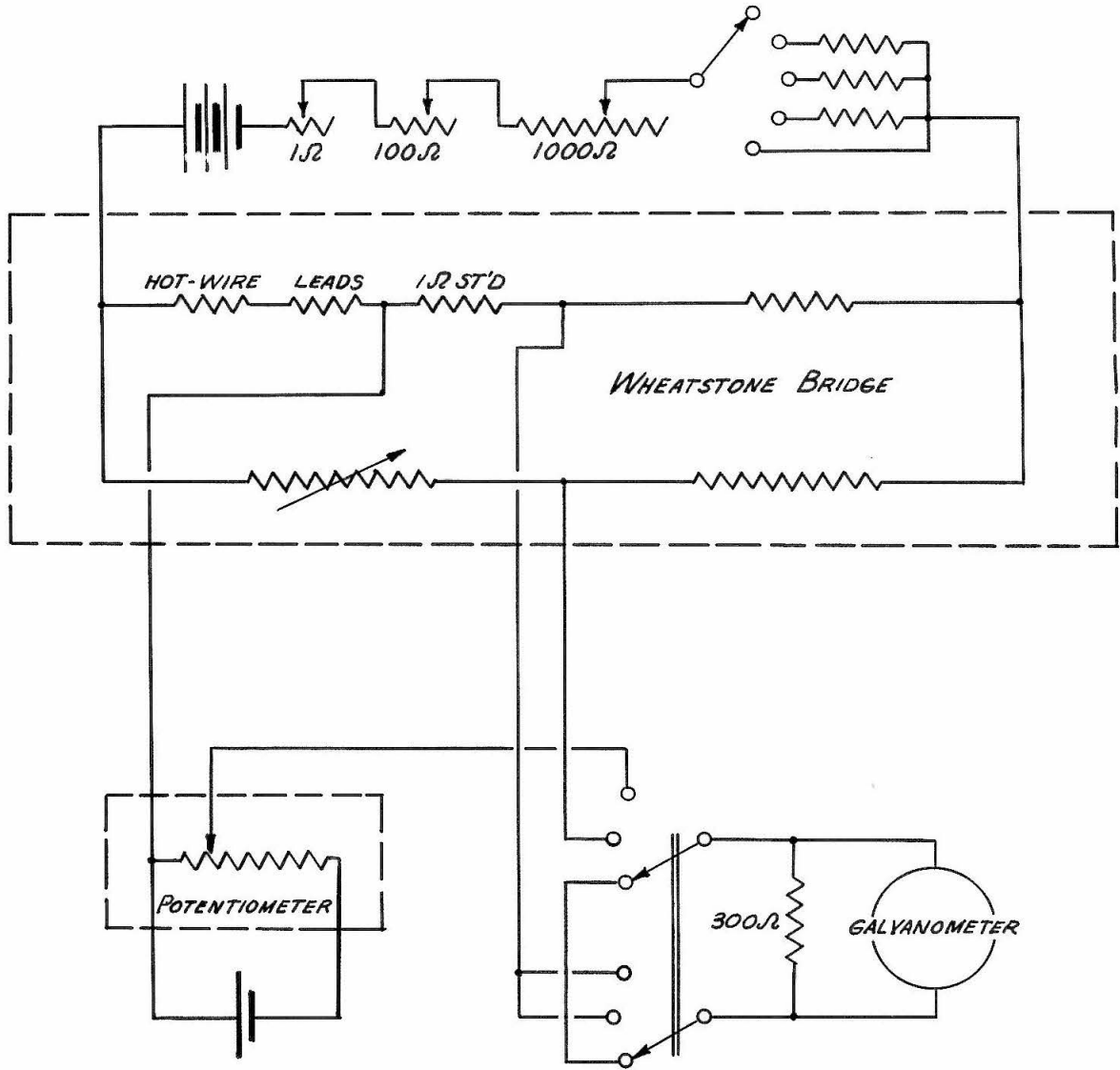
Standard Cell: Eppley Laboratory, Inc., Catalog No. 100
(was checked against two other standard cells in
use in the laboratory)

REFERENCES

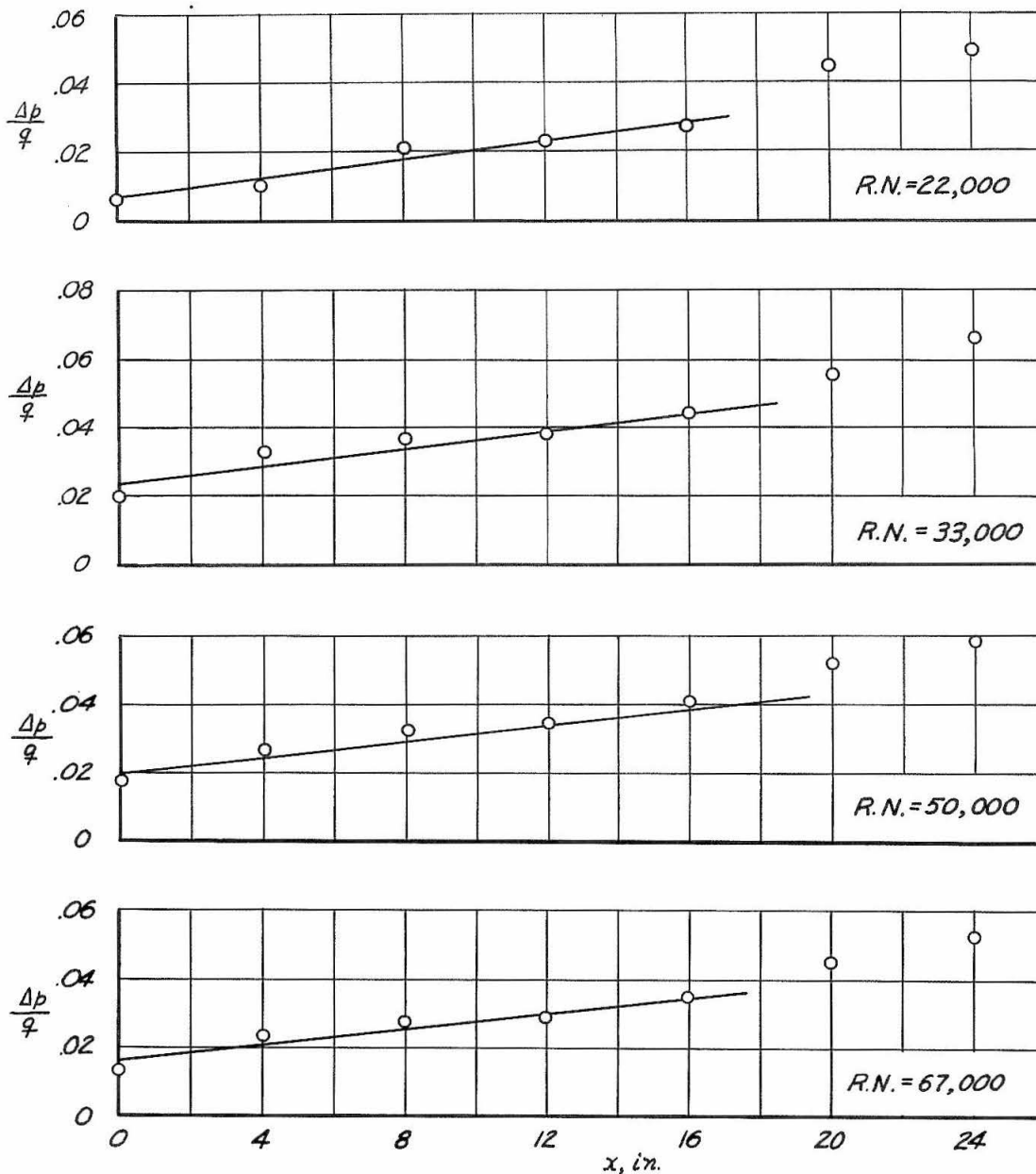
1. Laufer, J.: Investigations of Turbulent Flow in a Two-Dimensional Channel. NACA T.N. 2123.
2. Liepmann, H. W., Laufer, J. and Liepmann, K.: On the Spectrum of Isotropic Turbulence. To be published by the NACA.
3. Goldstein, S.: Modern Developments in Fluid Mechanics. Vol. II, Clarendon Press.
4. King, L. V.: On the Convection of Heat from Small Cylinders in a Stream of Fluid: Determination of the Convection Constants of Small Platinum Wires, with Applications to Hot-Wire Anemometry. Proc. Roy. Soc., Series A, Vol. 90, 1914.
5. Nikuradse, J.: Regularity of Turbulent Flow in Smooth Pipes. Translation. Technical Memorandum Pur-11. Purdue Research Foundation and Purdue University.
6. Dönch, F.: Divergente und Konvergente Turbulente Strömungen mit Kleinen Öffnungswinkeln. Forsch. Arb. Geb. Ing. Wes. Heft, 282, 1926.
7. Stanton, T. E. and Pannell, J. R.: Similarity of Motion in Relation to the Surface Friction of Fluids. Proc. Roy. Soc. 214, 1914.
8. Wattendorf, F.: Some Experimental Investigations of Flow in Curved Channels. Berkeley Meeting, Aeronautics and Hydraulics Division of A.S.M.E., June 1934.
9. Deissler, R. A.: Analytical and Experimental Investigation of Adiabatic Turbulent Flow in Smooth Tubes. NACA T.N. 2138.



THE TWO - DIMENSIONAL CHANNEL



SCHEMATIC CIRCUIT DIAGRAM OF HOT-WIRE EQUIPMENT

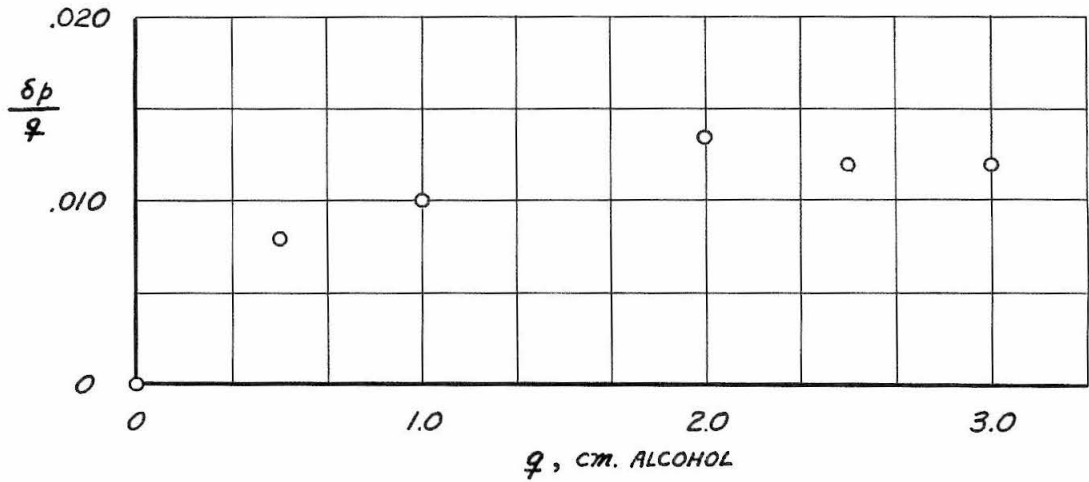


NOTE: q WAS MEASURED AT MID-CHANNEL.

CHANNEL EXIT IS AT $x = -5 \frac{7}{8}$ INCHES; FINAL PROFILES TAKEN AT $x = +7 \frac{7}{8}$ INCHES.

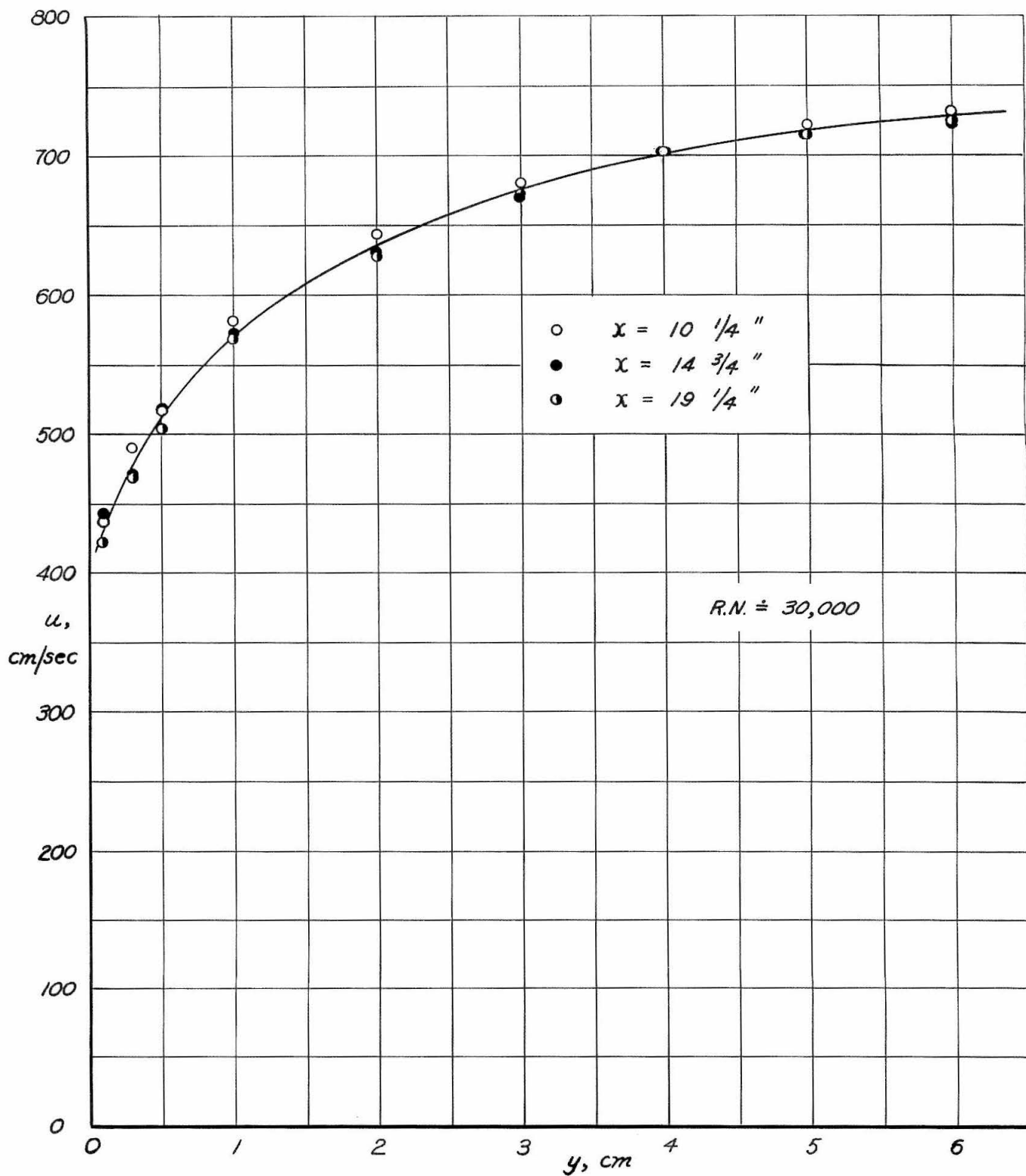
STRAIGHT LINES INDICATE SLOPES, AS INTERPOLATED FROM $\left(\frac{du}{dy}\right)_0$ VALUES.

PRESSURE ALONG THE CHANNEL AT $y = d$.

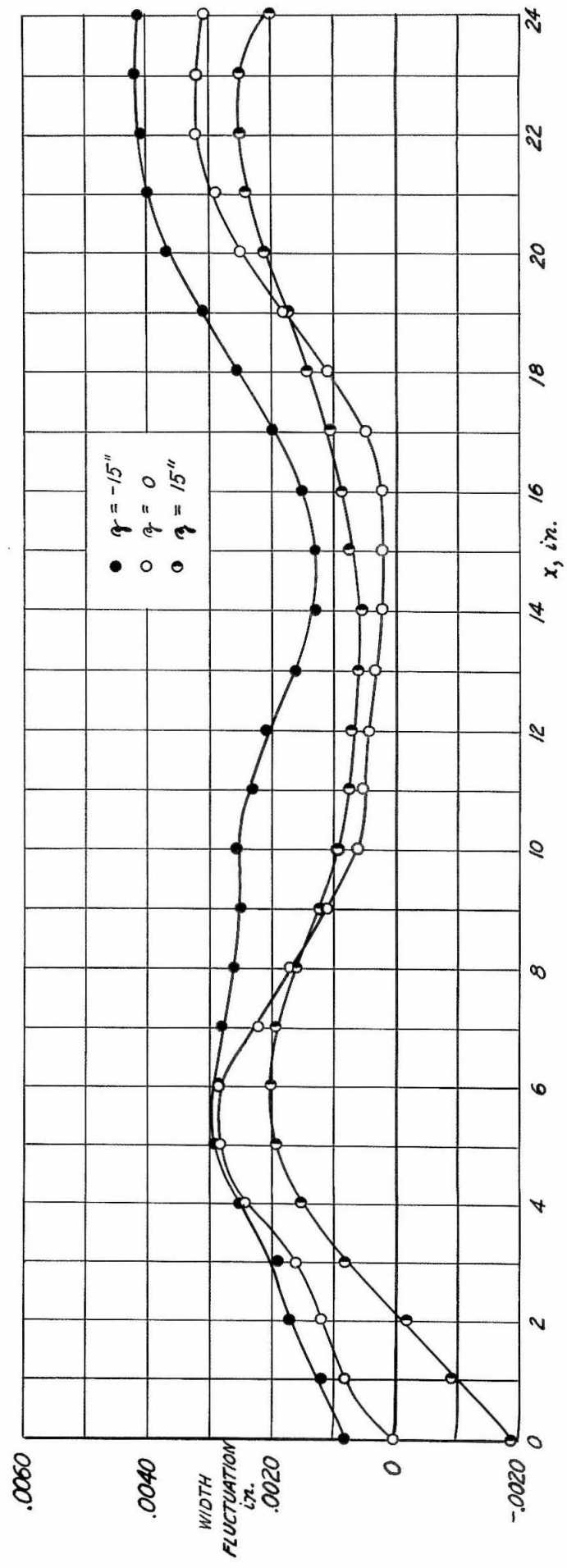


NOTE: δp = HEAD, IN cm. ALCOHOL, WHICH STATIC TUBE READS ABOVE ATMOSPHERIC PRESSURE.

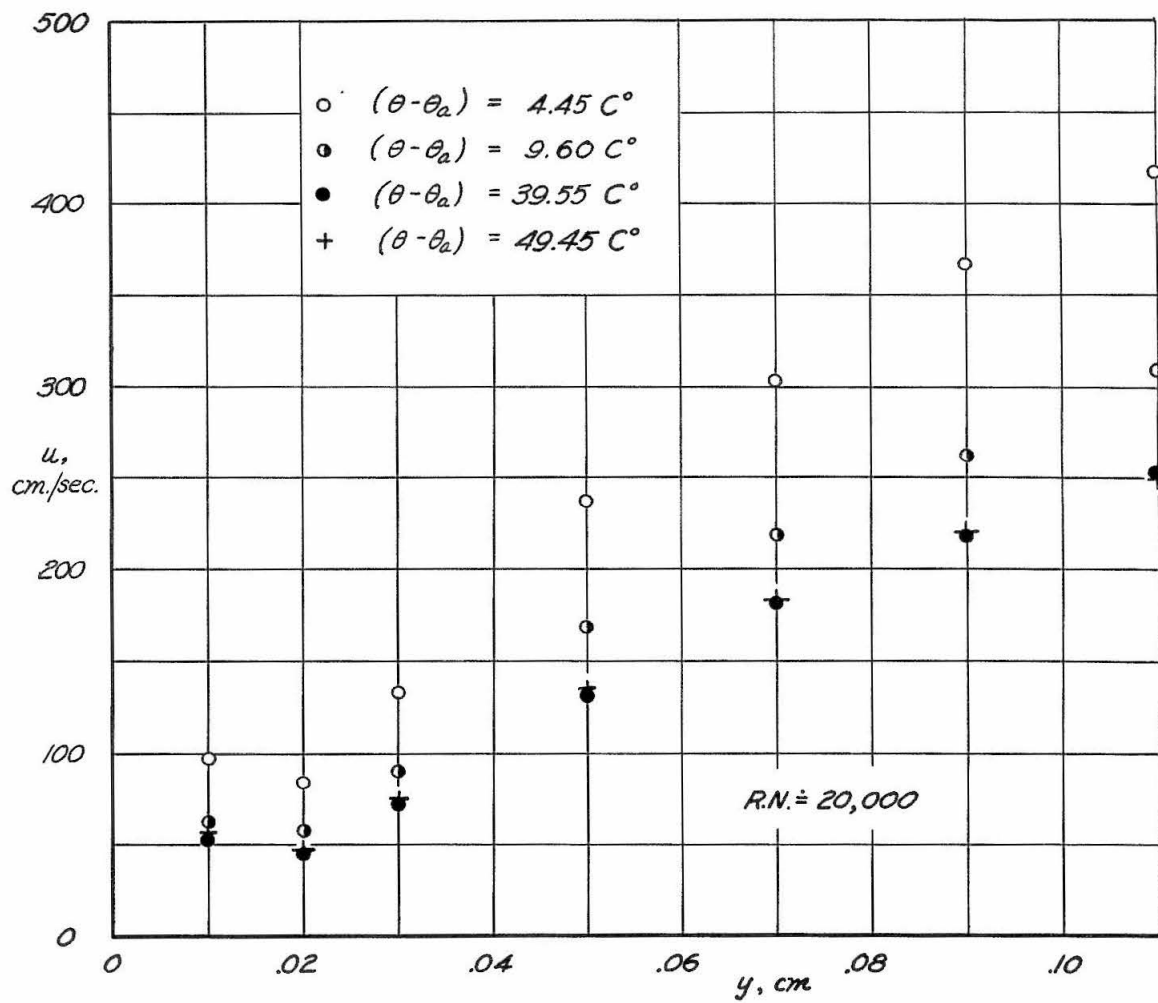
CHECK IN FREE JET OF STATIC TUBE USED FOR $\frac{dp}{dx}$ MEASUREMENTS



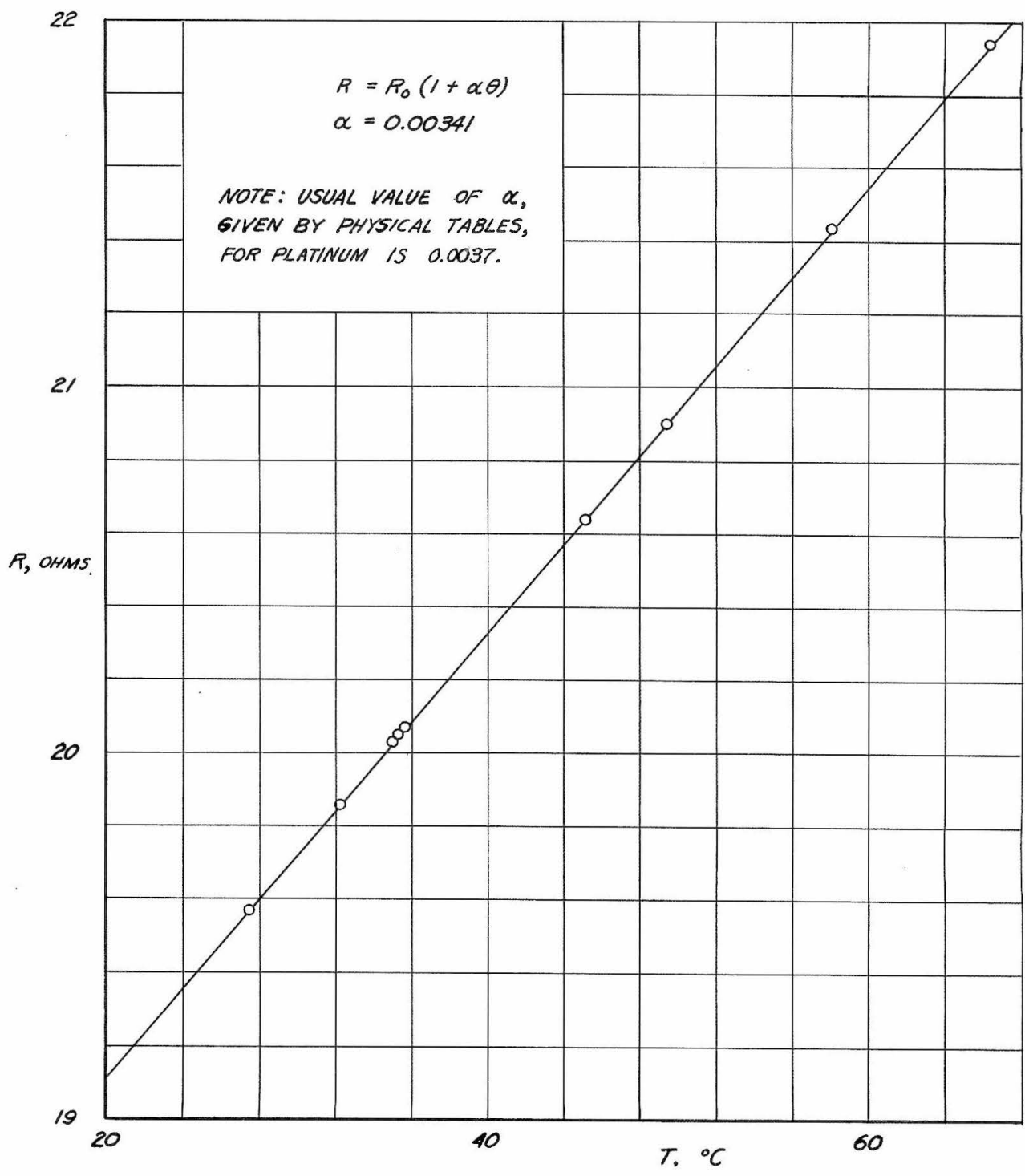
VELOCITY PROFILES AT THREE POSITIONS ALONG THE X-AXIS



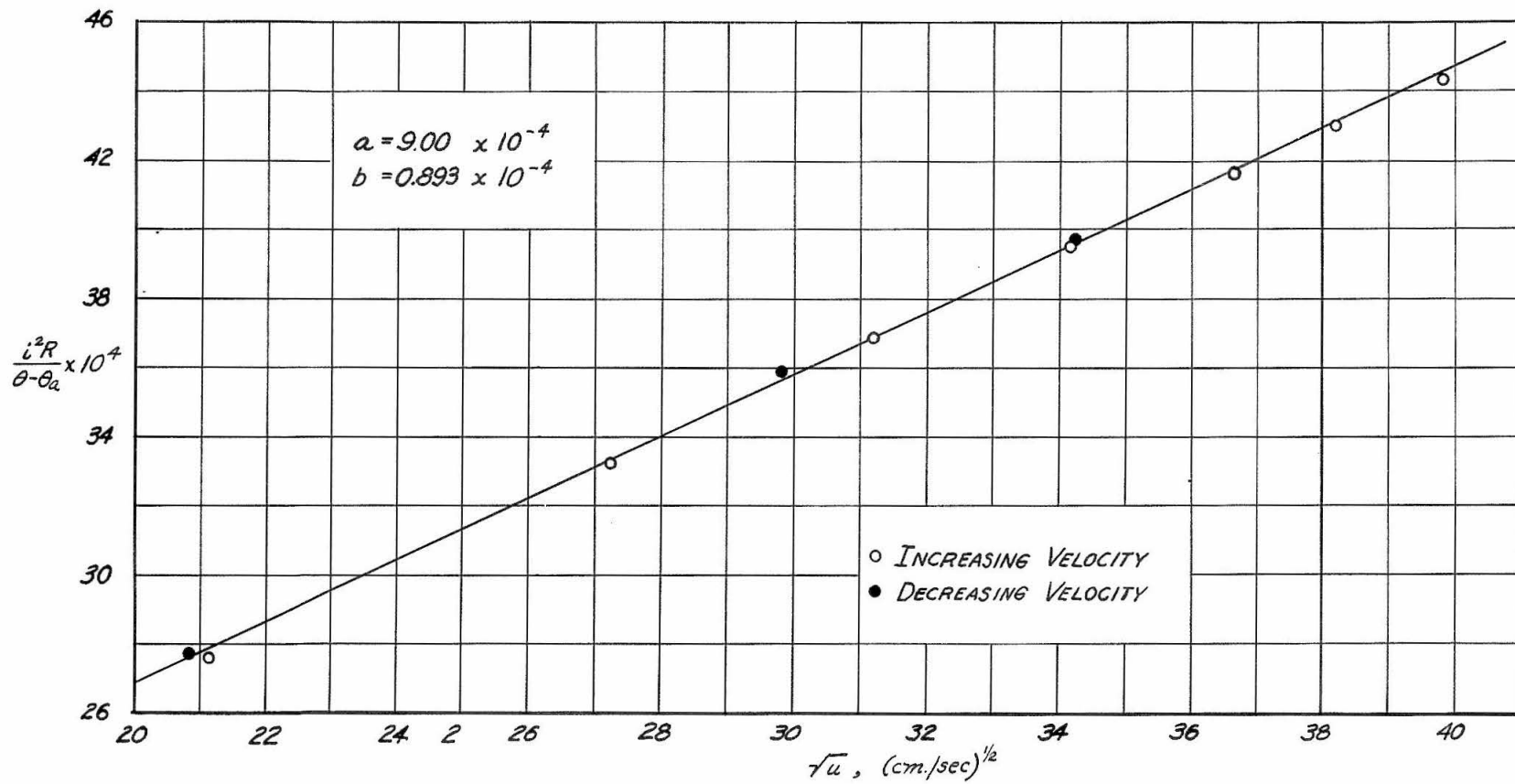
CHANNEL WIDTH FLUCTUATIONS FROM A NOMINAL VALUE OF APPROXIMATELY 5 INCHES



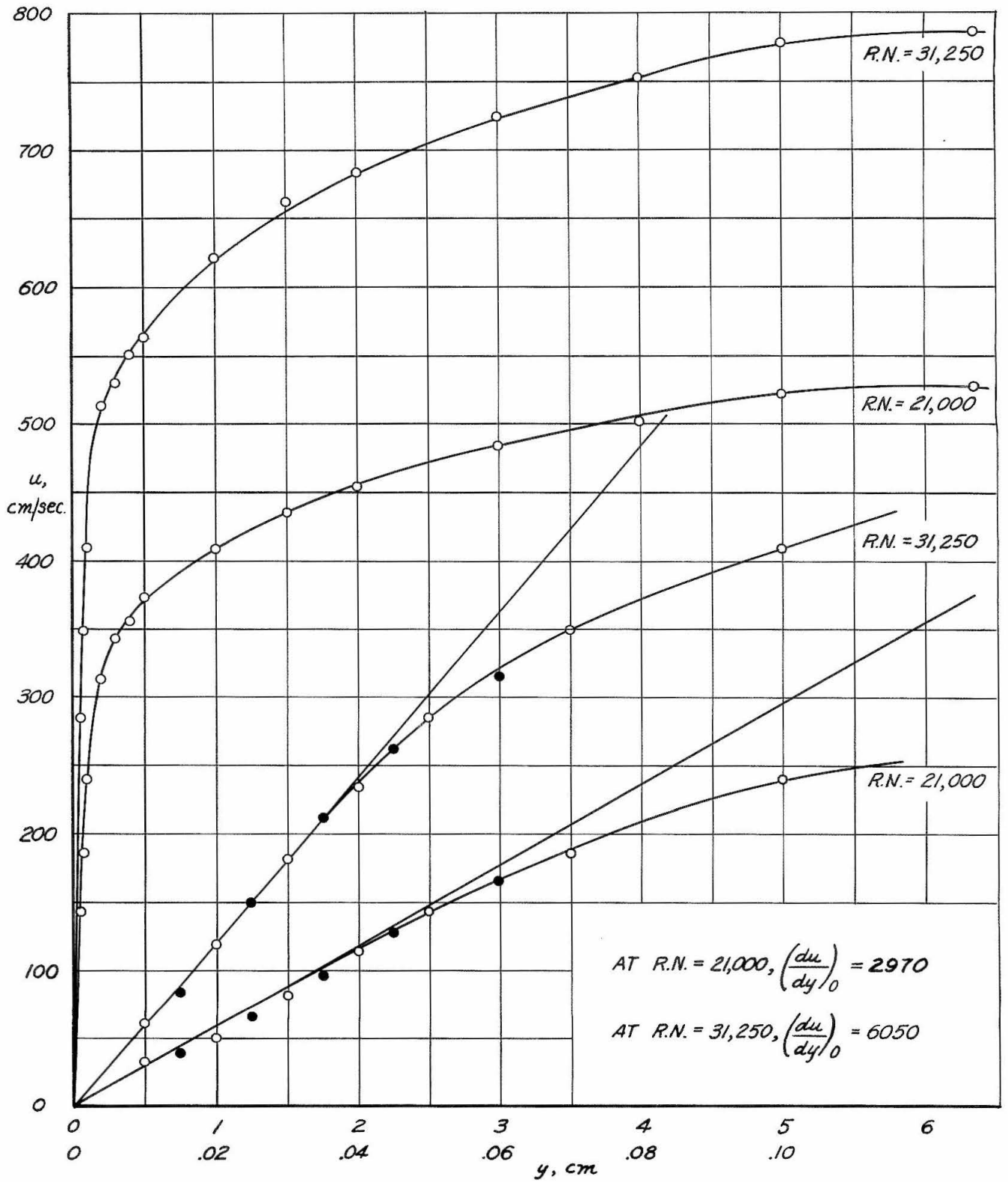
PROFILES OBTAINED BY OPERATING THE HOT-WIRE AT VARIOUS TEMPERATURES



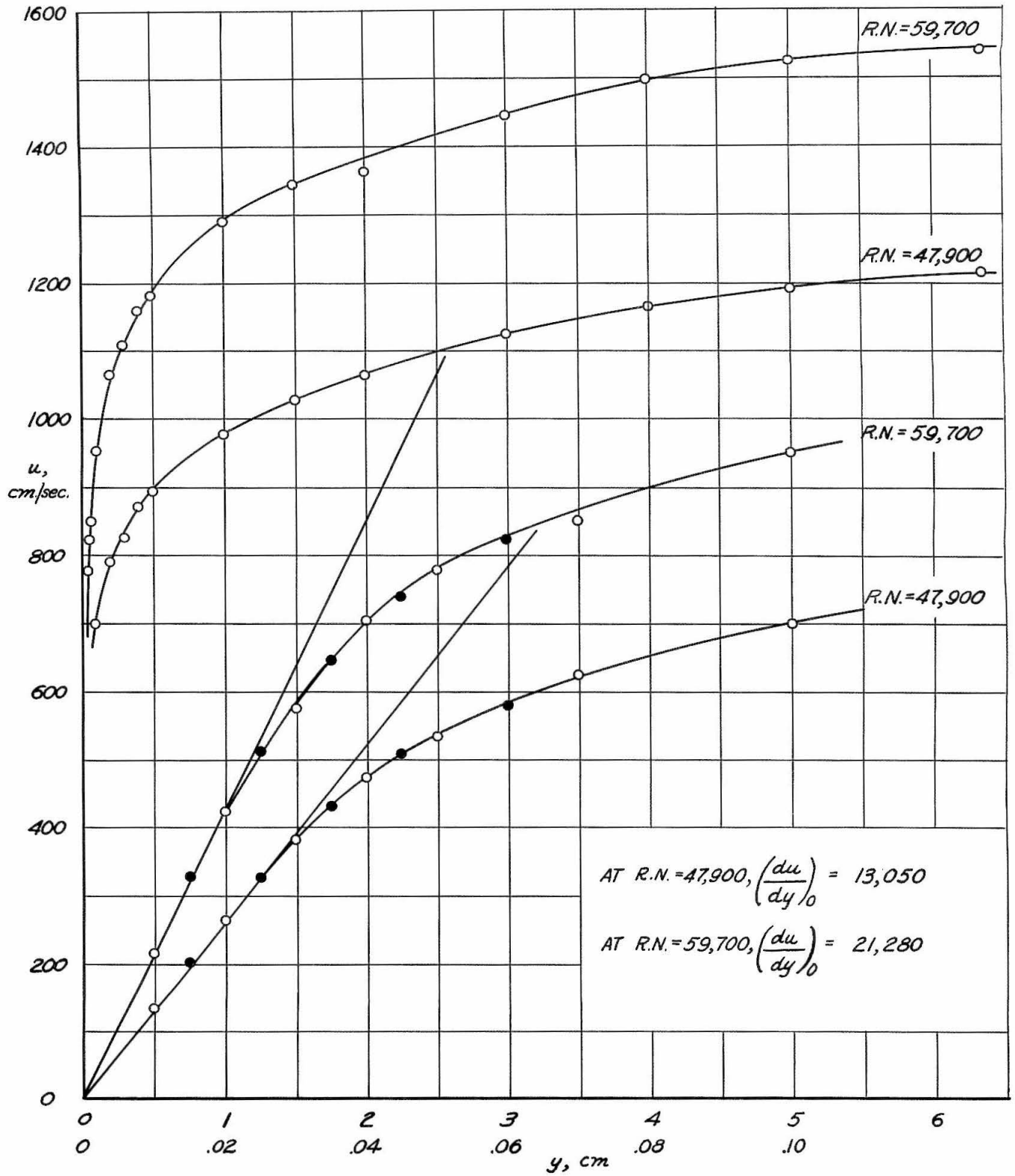
DETERMINATION OF α FOR THE HOT-WIRE USED FOR FINAL VELOCITY
PROFILE MEASUREMENTS



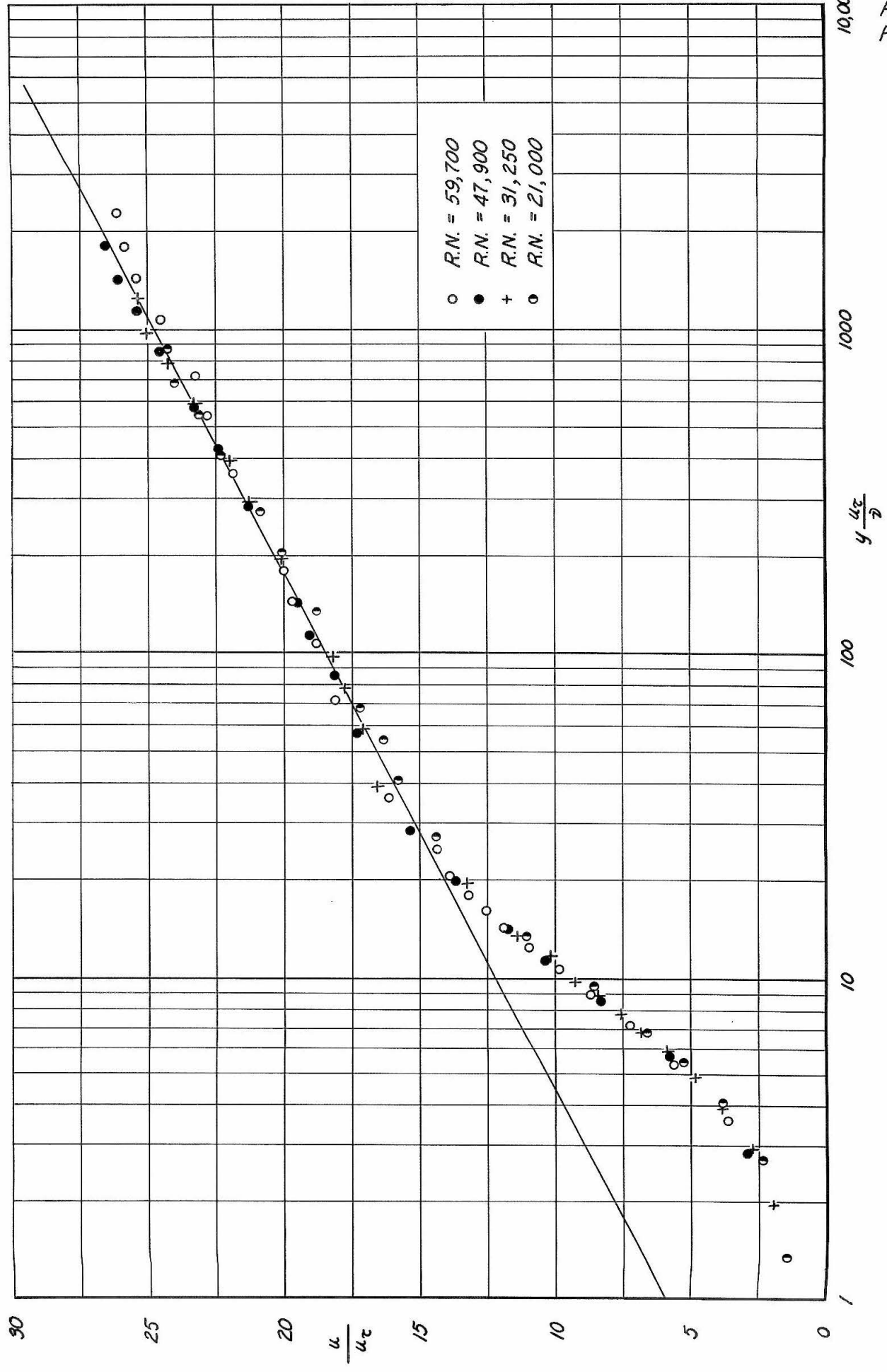
VELOCITY CALIBRATION OF THE HOT-WIRE USED FOR FINAL VELOCITY PROFILE MEASUREMENTS



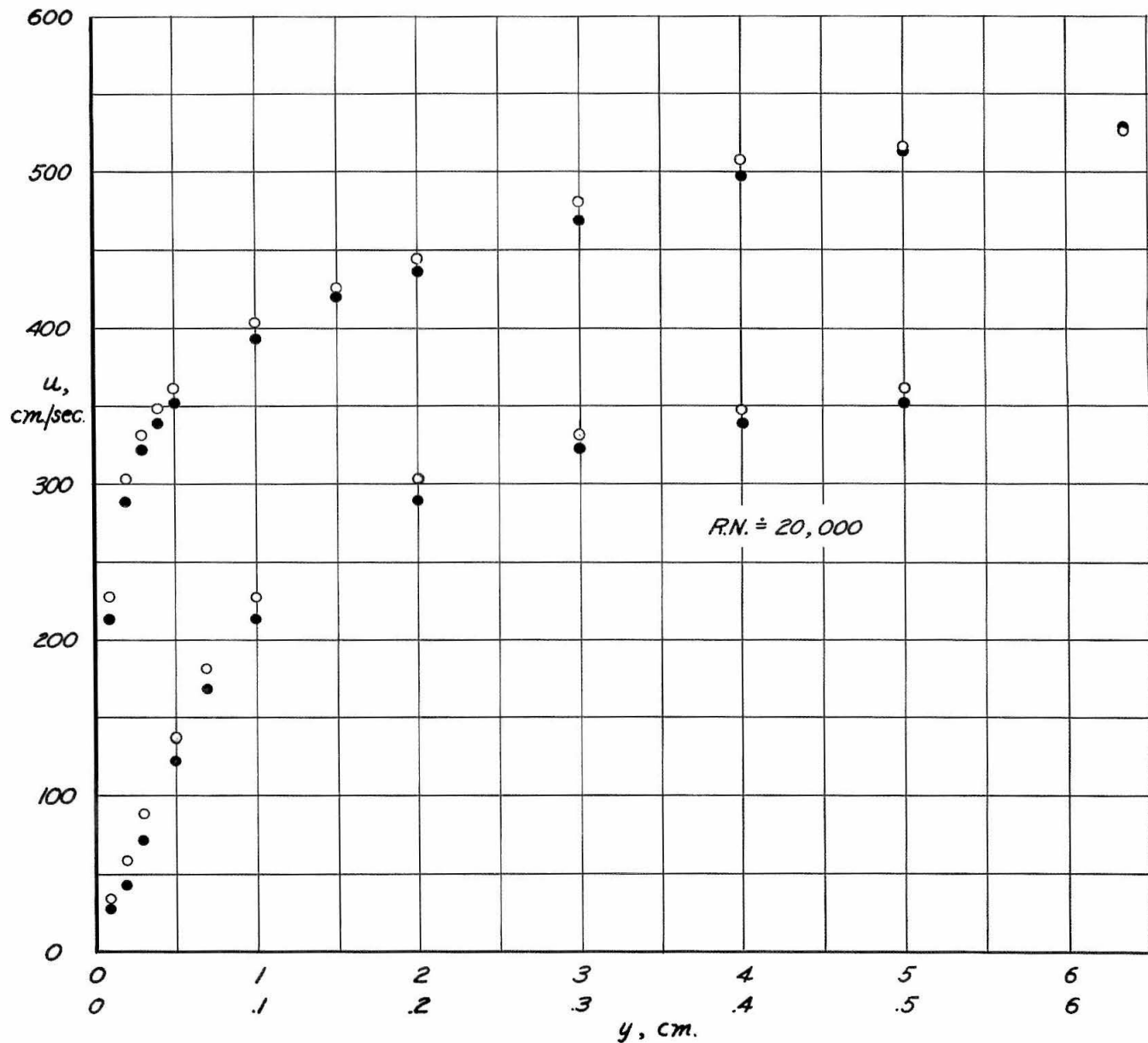
FINAL VELOCITY PROFILES AT R.N. = 31,250 AND 22,000



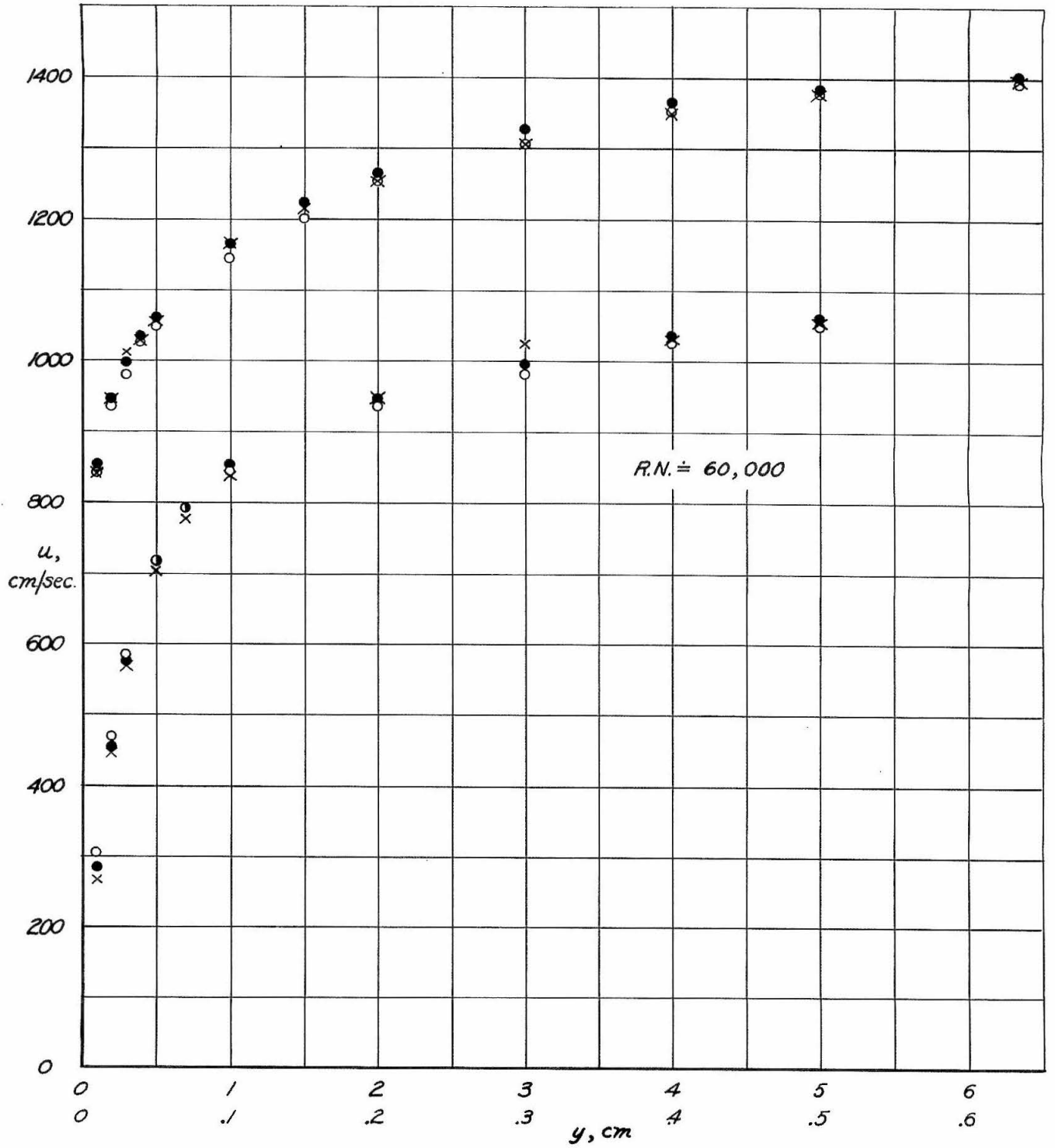
FINAL VELOCITY PROFILES AT $R.N. = 47,900$ AND $59,700$



DIMENSIONLESS SEMI-LOGARITHMIC PLOT OF FINAL VELOCITY PROFILES



EXAMPLE OF REPEATABILITY OF ABSOLUTE VELOCITY MEASUREMENTS AT THE LOWEST R.N.



EXAMPLE OF REPEATABILITY OF ABSOLUTE VELOCITY MEASUREMENTS AT THE HIGHEST R. N.